

Bioactive Polymer Fibers to Direct Endothelial Cell Growth in a Three-Dimensional Environment

Afra Hadjizadeh,^{†,‡} Charles J. Doillon,^{§,||} and Patrick Vermette^{*,†,‡}

Laboratoire de Bioingénierie et de Biophysique de l'Université de Sherbrooke, Department of Chemical Engineering, Université de Sherbrooke, 2500 University Boulevard, Sherbrooke, Québec, Canada, J1K 2R1, Research Center on Aging, Geriatric Institute, Sherbrooke University, 1036 rue Belvédère Sud, Sherbrooke, Québec, Canada, J1H 4C4, Oncology and Molecular Endocrinology Research Center, CHUL Research Center, 2705 Laurier Boulevard, Québec, G1V 4G2, Québec, Canada, and Department of Surgery, Faculty of Medicine, Laval University, Québec, G1K 7P4, Québec, Canada

Received October 4, 2006; Revised Manuscript Received December 17, 2006

This study reports the fabrication of bioactive polymer fibers onto which signaling molecules can control and direct cell responses. To encourage and control directional biological responses, GRGDS peptides were immobilized onto the surface of 100 μm diameter poly(ethylene terephthalate) (PET) fibers (monofilaments). PET fiber surfaces were first coated with a thin polymeric interfacial bonding layer bearing amine groups by plasma polymerization. Carboxy-methyl-dextran (CMD) was covalently grafted onto the surface amine groups using water-soluble carbodiimide chemistry. GRGDS were covalently immobilized onto CMD-coated fiber surfaces. X-ray photoelectron spectroscopy (XPS) analyses enabled characterization of the multilayer fabrication steps. Human umbilical vein endothelial cells were seeded and grown on fibers to investigate cell patterning behavior (i.e., adhesion, spreading, cytoskeleton organization, and cell orientation). Cell adhesion was reduced on CMD-coated fibers, whereas amine- and GRGDS-coated fibers promoted cell adhesion and spreading. Cell adhesion was enhanced as the GRGDS concentration increased. Epifluorescence microscopic visualization of cells on RGD-coated substrates showed well-defined stress fibers and sharp spots of vinculin, typical of focal adhesions. In comparison to plasticware commonly used in cell cultures, fiber curvature promoted cell orientation along the fiber axis.

Introduction

It is generally recognized that the behaviors of different cell types on polymeric materials depend largely on chemistry, topography, and mechanical properties at the cell–biomaterial interface.^{1–6} Most cell types are known to orient and often move rapidly along fibers in the 5–108 μm range, which has been referred to as contact guidance.^{7,8} Surface topography, as well as fiber curvature, is of particular interest to modulate the patterning of cells such as their proliferation and migration in 3-D environments.^{5,7,8}

However, on contact with complex multicomponent biological media, spontaneous protein adsorption occurs on the surfaces of synthetic biomaterials with heterogeneous biofilm formation typically comprised of various proteins. Recent biomaterial research aims to overcome the lack of selectivity in this initial adsorption of biological molecules onto synthetic surfaces. A promising route toward achieving controlled and predictable biomedical responses is to pre-coat a biomaterial surface with a layer of a desired protein or other biologically active molecules that can exert predictable biomedical responses.^{9–14} To modify biomaterial surfaces, bioactive ligands such as small peptide sequences may be either adsorbed or covalently grafted onto the surfaces of the biomaterials or included in their bulk composition.¹¹

Covalent immobilization of biologically active molecules onto polymer surfaces can often lead to a significant reduction in

the activity of the immobilized molecules. To avoid this problem, a spacer layer is often inserted between the substrate surface and the bioactive molecule,¹¹ preferably one with low nonspecific protein adsorption properties (e.g., poly(ethylene oxide) (PEG), carboxy-methyl-dextran (CMD), and partially amino-functionalized dextrans).^{13,15,17}

Many studies have investigated surface modification of 2-D substrates with cell-adhesive and non-cell-adhesive coatings.^{9–16} On the other hand, very few studies report ways to activate surfaces with biological molecules that can be applied in tissue engineering for 3-D tissue cultures, with the aim, for instance, of directing cell responses and tissue development by providing selective surface chemistry in a 3-D environment. Bio-activated fibers could be used to modulate cell patterning when dispersed in a 3-D environment. Only a few studies have reported cell orientation along small fibers.^{5,7,8}

The objective of this study was to develop and characterize bioactive polymer fibers that can encourage and control directional biological responses within 3-D environments. For this purpose, a thin polymeric interfacial bonding layer bearing amine groups was deposited onto 100 μm diameter PET fibers by radio frequency glow discharge (RFGD) deposition. Plasma polymerization of *n*-heptylamine was carried out in a custom-built plasma reactor. This method is known to deposit a cross-linked organic thin film with functional groups.^{17–19} Afterward, carboxy-methyl-dextran (CMD) was covalently grafted onto fibers bearing amine groups using water-soluble carbodiimide chemistry.^{1–3} GRGDS peptides were covalently immobilized onto CMD-coated fibers also by using carbodiimide chemistry.^{11,15,20,21} CMD is a polysaccharide with carboxyl groups that

* Corresponding author. Phone: +1 819 821 8000 ext. 62826. Fax: +1 819 821 7955. E-mail: Patrick.Vermette@USherbrooke.ca.

[†] Department of Chemical Engineering, Sherbrooke University.

[‡] Geriatric Institute, Université de Sherbrooke.

[§] CHUL Research Center.

^{||} Laval University.

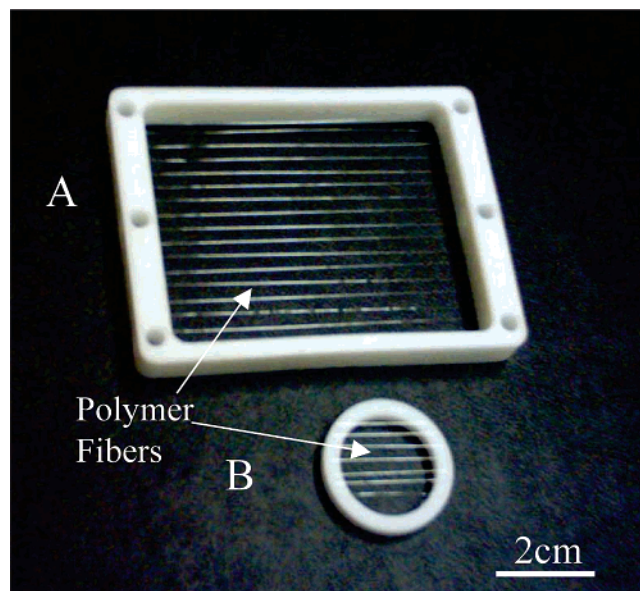


Figure 1. (A) Picture of the square holder used to keep polymer fibers (single filaments) within the plasma zone to modify fiber surfaces and subsequently to carry out XPS analyses. (B) Picture of the circular holder used to keep single filaments within the plasma zone to modify fiber surfaces to be subsequently used in cell culture testing.

can be used as a spacer to covalently link bioactive compounds and as a low-fouling layer to limit nonspecific protein adsorption.³

Human endothelial cells were derived from the umbilical cord vein (HUVEC) and used to investigate cell patterning (i.e., adhesion, spreading, cytoskeleton organization, and cell orientation) as a function of the fiber surface properties.

Materials and Methods

Materials. Commercially available 100 μm diameter monofilaments made of poly(ethylene terephthalate) (PET, cat. ES305910, Good fellow, Devon, UK) were used. PET fibers have been selected because of their commercial availability in monofilaments, their amenability to sustain the multistep surface modification used in this study, their biocompatibility, and their resistance toward standard autoclaving sterilization methods.

Borosilicate glass substrates were purchased from Chemglass (Vine-land, NJ). *N*-Heptylamine (99% purity) used in plasma polymerization was obtained from Sigma-Aldrich (cat. 51958, St. Louis, MO). Dextrans of 70 and 500 kDa molecular weights were purchased from Amersham Bioscience (cat. US14495, Uppsala, Sweden). Dextrans were carboxy-methylated to ca. 50% following a procedure similar to the work of Löfas and Johnsson.²² Briefly, CMD with ratios of carboxyl groups to anhydroglycopyranoside rings of 1:2 were prepared by dissolving 10 g of dextran in 50 mL of 2 M NaOH containing 1 M bromoacetic acid. The solution was stirred overnight and dialyzed against water for 24 h, then against 0.1 M HCl for 24 h, and finally for 24 h against water. The degree of carboxylation was assessed using NMR. The experimentally determined ratios were ca. one carboxyl group per two sugar units. GRGDS (cat. 44–0-23) and GRGES (cat. 44–0-51) peptides were purchased from American Peptide Company (Sunnyvale, CA).

PET Fiber Preparation. PET fibers were fixed onto nonconductive 3 mm thick Teflon frames [5 cm \times 7 cm square holder (Figure 1A) and a 2 cm diameter circular holder (Figure 1B)] to hold fibers steady in the plasma zone. The square frame was used to facilitate sample preparation (5 cm length fibers) for XPS characterization. The circular frame was designed for cell cultures in 12 multiwell plates. Fibers

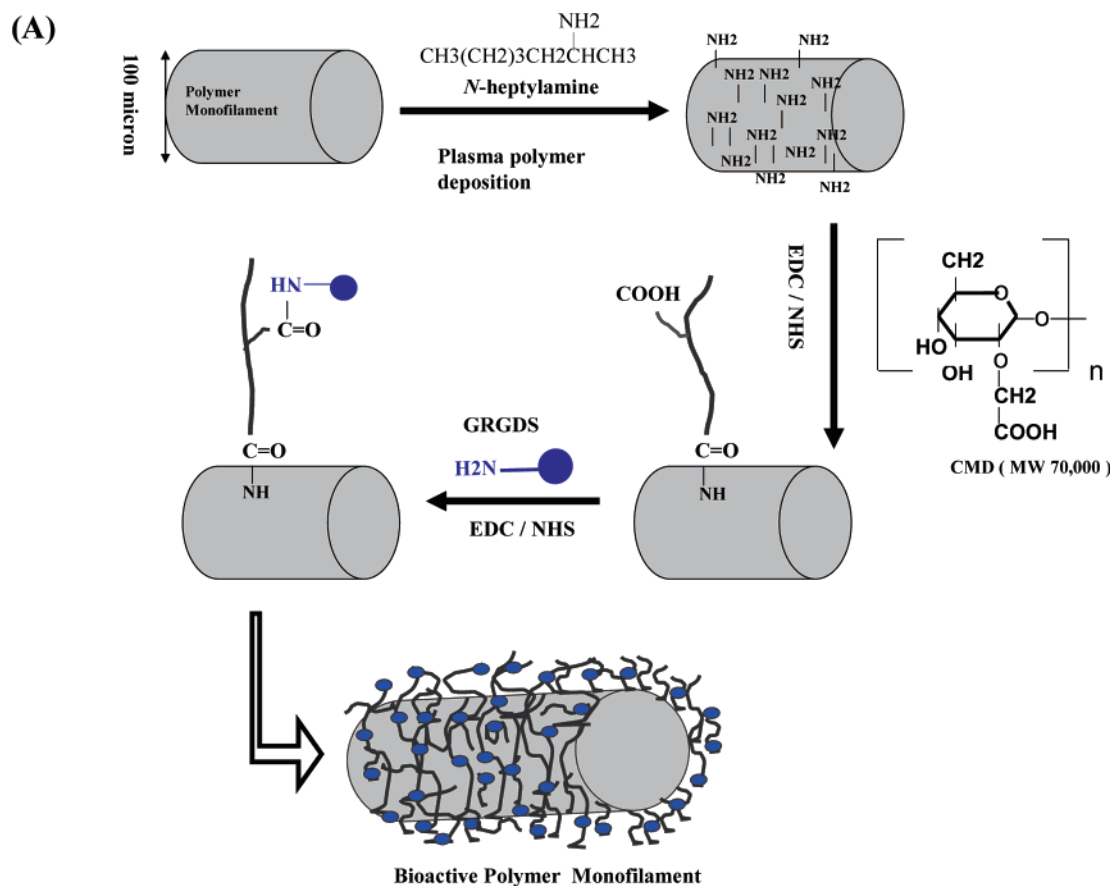
secured onto the frames were cleaned by an overnight incubation into a surfactant solution (RBS Detergent 35, Pierce Biotechnology, Rockford, IL, cat. 27952). Then, fibers were sonicated for 10 min in RBS solution followed by 10 min in ethanol (ACS grade). Scanning electron microscope (SEM) analyses of the PET fibers exposed to such a sonication procedure revealed no damage to the PET monofilaments. Fibers were thoroughly rinsed under a flow of Milli-Q water (with a resistivity of not less than 18.2 M Ω cm) and blow-dried using 0.2 μm filter-sterilized compressed air.

Deposition of Reactive Amine Groups onto PET Fibers by Plasma Polymerization. PET fibers firmly fixed to the holders were first activated using plasma Radio Frequency Glow Discharge (RFGD) deposition to obtain a cross-linked polymeric thin film with surface reactive groups (Figure 2) onto which further layers could be immobilized by aqueous phase chemistry.¹⁹ The reactor employed for plasma polymerization was a custom-built batch reactor in which plasma was produced in a vacuum by a radio frequency supply. The holders bearing the fibers were placed on the lower circular electrode, which has a diameter of 9.5 cm. Deposition of thin plasma polymer films was carried out from the vapor of *n*-heptylamine as described elsewhere.¹⁹ Parameters selected for the plasma deposition of *n*-heptylamine were a frequency of 50 kHz, a load power of 80 W, and an initial monomer pressure of 0.040 Torr. Deposition time was set to 70 s, and the distance between the electrodes was set at 10 cm.

CMD Immobilization onto Plasma-Modified PET Fibers. CMD was attached directly to *n*-heptylamine plasma polymer (HApp)-coated fibers using water-soluble carbodiimide chemistry.³ One and 2 mg/mL CMD solutions were prepared in Milli-Q water. Once dissolved, 19.2 mg/mL 1-ethyl-3-(3-dimethylaminopropyl) carbodiimide (EDC) and 11.5 mg/mL *N*-hydroxysuccinimide (NHS) were added to the CMD solutions. Holders bearing HApp-coated monofilaments were then immersed in this solution and left to react overnight at room temperature under vigorous agitation. To remove any noncovalently attached CMD, the fibers were rinsed for 24 h under vigorous agitation in a 1 M NaCl solution, followed by an immersion in Milli-Q water for 24 h under agitation at room temperature before again being rinsed in Milli-Q water and subsequently used.

Peptide Grafting onto CMD-Coated Fibers. GRGDS and GRGES immobilization was carried out according to a sequential procedure similar to the ones described elsewhere.^{11,15,20,21} To avoid any potential damage of the GRGDS and GRGES peptides during the sterilization of the PET monofilaments prior to cell culture, peptide immobilization was performed under sterile conditions using pre-sterilized CMD-coated fibers. CMD-coated fibers were placed in Milli-Q water and autoclaved at 121 $^{\circ}\text{C}$ for 25 min. Then, sterile fibers were immersed into filter-sterilized (low binding 0.22 μm syringe filters, Millipore Corporation, Bedford, MA) solutions of EDC (19.2 mg/mL) and NHS (11.5 mg/mL) in PBS (1 \times , pH 7.4) at room temperature for 4 h, followed by rinsing with PBS (pH 7.4; 2 \times 15 min). The fibers were then incubated into a filter-sterilized (0.22 μm) peptide solution of 0.1, 0.5, or 1 mg/mL GRGDS or GRGES made in PBS (pH 8) for 2–3 h at room temperature. After being rinsed with PBS (pH 8, 3 \times 15 min) to remove unbounded free peptides, fibers were left to dry under a sterile hood. The advantage of this sequential procedure is that it limits intra- and/or intermolecular condensation of the RGD peptides. Using this two-step procedure, the carboxyl groups of the aspartate side chain are not activated and are therefore not available for coupling. Also, protonation of the arginine side chain in water was nearly abolished.

Surface Characterization of Polymer Fibers by X-ray Photoelectron Spectroscopy (XPS). XPS analyses were performed using an AXIS HS spectrometer (Kratos Analytical, Manchester, UK) equipped with a monochromatic Al K α source at a power of 120 W. The total pressure in the main vacuum chamber during analysis was typically 2 \times 10^{−8} mbar. Elements present were identified from survey spectra. For further analysis, high-resolution spectra were recorded from individual peaks at 40 eV pass energy. Atomic concentrations of each element were calculated by determining the relevant integral peak area



(B)

G-R-G-D-S (Gly-Arg-Gly-Asp-Ser): $(\text{C}_2\text{H}_5\text{NO}_2)-(\text{C}_6\text{H}_{14}\text{N}_4\text{O}_2)-(\text{C}_2\text{H}_5\text{NO}_2)-(\text{C}_4\text{H}_7\text{NO}_4)-(\text{C}_3\text{H}_7\text{NO}_3)$

G-R-G-E-S (Gly-Arg-Gly-Glu-Ser): $(\text{C}_2\text{H}_5\text{NO}_2)-(\text{C}_6\text{H}_{14}\text{N}_4\text{O}_2)-(\text{C}_2\text{H}_5\text{NO}_2)-(\text{C}_5\text{H}_9\text{NO}_4)-(\text{C}_3\text{H}_7\text{NO}_3)$

Figure 2. (A) Schematic diagrams (not to scale) of the methods used for the covalent surface immobilization of GRGDS and GRGES peptides via an *n*-heptylamine plasma polymer (HApp) and carboxy-methyl-dextran (CMD) interlayers. (B) Chemical sequence of the GRGDS and GRGES peptides.

(using a Shirley-type background) and applying the sensitivity factors supplied by the instrument manufacturer. The random error associated with elemental quantification has been determined, for this instrument, to be 1–2% of the absolute values for atomic percentages >5%. A value of 285 eV for the binding energy of the main C 1s component (CH_x) was used to correct for charging of specimens under irradiation.

Assuming a value of ≈ 3 nm for the electron attenuation length of a C 1s photoelectron in a polymeric matrix, this translates into an approximate value for the XPS analysis depth (from which 95% of the detected signal originates) of 10 nm when recording XPS data at an emission angle normal to the surface.

Cell Culture. Human umbilical vein endothelial cells (HUVECs) were isolated from human umbilical cord veins as previously described.²³ HUVECs were cultured in M199 culture medium (cat. M5017, Sigma-Aldrich, St. Louis, MO) containing 2.2 mg/mL sodium bicarbonate (Fisher, Fairlawn, NJ), 90 $\mu\text{g}/\text{mL}$ sodium heparin (cat. H1027, Sigma-Aldrich, St. Louis, MO), 100 U/100 $\mu\text{g}/\text{mL}$ penicillin/streptomycin (cat. 15140–122, Invitrogen Corporation, Grand Island, NY), 10% fetal bovine serum (FBS, cat. F1051, Sigma-Aldrich, St. Louis, MO), 2 mM L-GLUTAMINE (CAT. 25030149, INVITROGEN CORPORATION, GRAND ISLAND, NY), AND 25 MG/ML ENDOTHELIAL GROWTH FACTOR SUPPLEMENT (ECGS, CAT. 356006, BD BIOSCIENCES, SAN JOSE, CA).

Cell Seeding onto Surface-Modified Fibers. Cell cultures on the different PET fibers were carried out by adapting procedures described elsewhere.^{9,24–26} To evaluate the effect of surface-modified polymer

fibers on HUVEC responses and patterning, fibers were positioned in parallel direction onto a circular Teflon holder (2 cm in diameter, Figure 1B). On this holder, fibers were distanced approximately 0.5–2 mm from each other. Fibers were then surface-modified and subsequently sterilized directly onto the holders; non-coated PET fibers, HApp-, and CMD-coated fibers were placed in Milli-Q water and autoclaved at 121 °C for 25 min. Three specimens of uncoated cleaned PET monofilaments and PET monofilaments coated with (1) HApp, (2) HApp + CMD, (3) HApp + CMD + GRGDS, and (4) HApp + CMD + GRGES layers were investigated. Holders bearing the fibers were placed into wells of 12-well tissue culture polystyrene (TCPS) plates, then rinsed in sterile PBS (pH 7.4), and incubated in M199 culture medium for 1–2 h to keep fibers hydrated until cells were seeded. Then, 1 mL of M199 culture medium containing 1×10^6 cells was directly poured into the well containing the fiber holder. Cells of passages of 3–5 were used in all experiments. Fibers were incubated for 1 h and agitated. Afterward, the holders bearing the fibers were transferred into new 12-well TCPS plates containing fresh M199 culture media and incubated in a CO_2 incubator at 37 °C and 5% CO_2 . Controls were carried out with the same cells grown directly on the plastic surface of the 12-multiwell TCPS plates.

Cell Attachment Assessment. Cell attachment assessment was performed following a 4 h incubation period.^{10,11} The culture media were removed from the wells, and cells were incubated with Hoechst 33258 (cat. H1398, Molecular Probes Inc., Burlington, Canada) at a concentration of 10 $\mu\text{g}/\text{mL}$ in a fresh M199 culture medium for 30

Table 1. Elemental Compositions of PET Fiber Surfaces Obtained by XPS Analyses

samples	atomic concentrations (%) \pm SD			atomic ratios (%)		exposure to oxygen
	C 1s	O 1s	N 1s	N/C	O/C	
PET fibers	73.4 \pm 2.1	26.6 \pm 2.3	0.0 \pm 0.0	0.000	0.36	NA
PET + HApp	88.1 \pm 0.0	2.5 \pm 0.6	8.7 \pm 0.5	0.098	0.03	1 h
PET + HApp + CMD (1:2, ^a 70 kDa, 1 mg/mL)	75.8 \pm 1.8	18.2 \pm 0.5	6.0 \pm 1.3	0.079	0.24	3 days
PET + HApp + CMD (1:2, 70 kDa, 2 mg/mL)	77.4 \pm 0.6	17.8 \pm 0.6	4.8 \pm 0.7	0.062	0.23	3 days
PET + HApp + CMD (1:2, 70 kDa, 2 mg/mL) following autoclave	80.1 \pm 0.9	14.0 \pm 1.5	5.4 \pm 0.2	0.068	0.18	3 days
PET + HApp + CMD (1:2, 500 kDa, 1 mg/mL)	77.2 \pm 0.3	17.1 \pm 0.6	5.7 \pm 0.2	0.073	0.22	3 days
PET + HApp + CMD (1:2, 500 kDa, 2 mg/mL)	77.1 \pm 1.7	18.1 \pm 0.1	6.0 \pm 1.7	0.078	0.24	3 days
PET + HApp + CMD (1:2, 70 kDa, 2 mg/mL) + GRGDS (0.1 mg/mL)	78.0 \pm 3.5	16.8 \pm 3.2	5.2 \pm 0.4	0.067	0.22	5 days
PET + HApp + CMD (1:2, 70 kDa, 2 mg/mL) + GRGDS (0.5 mg/mL)	78.2 \pm 1.8	16 \pm 1	5.9 \pm 0.7	0.076	0.21	5 days
PET + HApp + CMD (1:2, 70 kDa, 2 mg/mL) + GRGDS (1 mg/mL)	71.8 \pm 2.0	21.8 \pm 0.1	6.4 \pm 0.6	0.089	0.30	5 days

^a 1:2 means a carboxylation degree of 1:2.

min. Samples were then observed under an inverted microscope (Nikon) using fluorescence and phase contrast imaging. Images were taken with a 10 \times lens in conjunction with a digital CCD camera (Regita 1300R, QIMAGING, Burnaby, Canada) and imaging software (SimplePCI, Compix Inc., Minneapolis, MN). The numbers of nuclei per fiber, corresponding to the number of attached cells, were counted using SigmaScan5 software. The average cell number was determined from $n = 18$, comparisons between sample groups were made using ANOVA, and data are reported as mean \pm standard deviation.

Assessment of Cell Spreading and Patterning. To monitor cell growth, cell spreading, and cell patterning, HUVEC-seeded fibers were kept in culture in an incubator (37 $^{\circ}$ C, 5% CO₂) for 4 h. The culture media were replenished every 2 days. For cell staining, cell-seeded fibers were gently washed with PBS (3 times) and fixed in a formaldehyde solution (3.75 wt %/v) in PBS for 15 min. Following three washings with PBS, cells adhered on fibers were then permeabilized using a Triton X-100 solution (0.5% v/v in PBS) (Sigma Chemical Co.) for 5 min. Following two rinses in PBS, the samples were incubated in a mixture of TRITC-phalloidin (1:100 dilution, cat. P1951, Sigma Chemical Co.) and SYTOX Green Nucleic Acid Stain (1 μ M, cat. S7020, Molecular Probes, Eugene, OR) or with Hoechst 33258 (1:100 dilution) in a blocking buffer solution (a solution containing bovine serum albumin (20% in PBS)) for 1 h at room temperature and in the dark. The staining solution was removed, and following washes with PBS (3 times), the preparations were then visualized on an Olympus Fluoview 300 confocal microscope and on an epifluorescence microscope (Nikon, Eclipse TE 2000-S). Images were captured using a COOLSNAP-Pro camera on Image-pro plus imaging software. The double-stain allowed us to adequately distinguish the cell cytoskeleton (i.e., actin filaments) and nuclei. All experiments were replicated two or more times. At least four fibers were examined for each sample.

The detailed examination of the acting filament and focal adhesion structures was very difficult directly on PET fibers because of the lack of transparency of these fibers. Therefore, borosilicate glass substrates were surface-modified and sterilized under the same experimental conditions as those used to surface activate PET fibers with the aim of gathering more information on the effect of the surface coatings on the actin filament and focal adhesion of the cells seeded on the different coatings.

Borosilicate glass substrates bearing the different surface coatings were placed in the wells of a 12-well culture plate. HUVECs were seeded onto these samples at a density of 10 000 cells/cm² and kept in culture, as for PET fibers, for 4 days. Afterward, the samples were fixed and permeabilized by the same procedure described previously and incubated for 1 h with a primary antibody (Monoclonal Anti-Vinculin, Sigma, cat. V4505) at a dilution of 1:25 in the same blocking buffer described previously. Samples were then washed 3 times with PBS for 5 min each and then incubated with the secondary antibody

(1:250 dilution of Anti-Mouse IgG, Sigma, cat. A2304) in the same blocking buffer for 1 h. Samples were washed twice with PBS (5 min each) and then mounted face-down onto glass microscope slides. Edges of the samples were sealed with nail polish and kept in the dark until epifluorescence microscopic observation. All experiments were replicated 2 or more times. At least four fields were examined for each sample to assess the degree of stress fiber and focal adhesion formation on each substrate.

To observe cell growth on the GRGDS (concentrations of 0.5 and 1 mg/mL)-coated fibers during a 10 day cell culture period, live cells were stained with dil-acetylated LDL (cat. BT-902, Biomedical Technologies Inc., Stoughton, MA) at day 2. Then, samples were observed with phase contrast or confocal microscopy every day.

Results and Discussion

Surface Analyses by XPS. As listed in Table 1, the successful surface modification of PET fibers by HApp, CMD, and GRGDS layers was immediately evident from the elemental composition determined by XPS analyses. XPS analyses of clean untreated PET fibers show C—C, C—O, and C=O components in the C 1s high-resolution spectra (Figure 3A) located at 285, 286.4, and 289 eV, respectively. This is in agreement with the PET fiber chemical composition and XPS analyses of PET fibers obtained from other studies.²⁷

XPS analysis of HApp layers on PET fibers (Figure 3B and Table 1) indicated a polymer rich in hydrocarbon- and nitrogen-containing species, as observed previously on different substrates.^{17,18,29} The broad C 1s peak is associated with the variety of chemical structures, formed during plasma deposition from the HApp layer. As a result it is difficult to clearly resolve the C—N-containing species from those containing C—O, which may result from the spontaneous quenching of carbon radicals within the film on exposure to air. The reduction in oxygen atomic concentration from 26.6% for an uncoated PET monofilament to 2.5% for a HApp-coated PET monofilament also indicates a uniform and thick plasma polymer layer. However, it is difficult to determine the thickness of the HApp layers based only on XPS analyses.

Surface modification by plasma polymerization has been applied extensively in the biomaterial field because the films produced are very smooth, pinhole and defect free, have good adhesive properties, can be deposited onto many different materials and complex geometries, and generally contain low amounts of leachables.^{18,28,30} This method has been also shown to produce uniform films across silicon wafers and glass substrates.¹⁹ But since plasma polymer films rapidly oxidize in

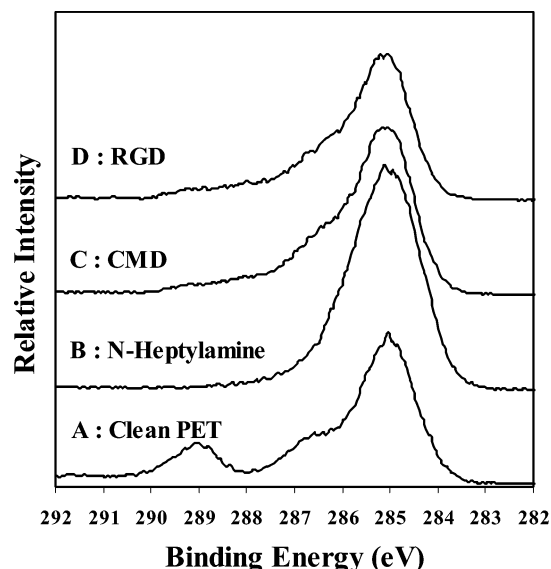


Figure 3. High-resolution XPS C 1s spectra of (A) clean untreated PET fibers, PET fibers coated with (B) HApp layer, (C) HApp + CMD (70 kDa) with a ratio of one carboxyl group to two sugar units produced from a 2 mg/mL CMD solution, and (D) HApp + CMD + GRGDS (0.5 mg/mL). The spectra have been displayed relative to each other in the Y-direction to allow comparison of peak positions.

air, they should be used immediately after preparation.^{19,28,30,31} The introduction of C—O (286.5 eV) and C=O (289 eV) observed in the high-resolution C 1s spectra indicated the successful grafting of carboxy-methyl-dextrans onto the HApp interlayer (as shown in Figure 3C). A nitrogen signal was still evident, indicating that the CMD coating (in the dry state) is much thinner than the XPS analysis depth. These results are in agreement with those of an earlier study using the same multilayer structure.³²

To examine the effect of CMD molecular weight and CMD solution concentration during the immobilization procedure on the CMD coating, CMDs of 70 and 500 kDa molecular weights and two CMD solution concentrations (1 and 2 mg/mL) were used. As depicted in Figure 4, the XPS surface chemical compositions of the four CMD coatings were similar. As a result, CMD-coated fibers produced using CMD of 70 kDa molecular weight with a carboxylation ratio of 1:2 and a CMD solution concentration of 2 mg/mL were selected for cell testing of these fibers.

To justify the application of these fibers in cell and tissue culture applications, they would need to sustain standard sterilization procedures. As autoclaving is often the preferred method of sterilization for biomedical devices, the effect of autoclaving on fiber coatings was examined by XPS. XPS analyses revealed a small change in the surface elemental composition of the CMD-coated fibers (Table 1). Although we took good care to thoroughly rinse the CMD-coated fibers with a 1 M NaCl solution following CMD immobilization to remove physisorbed CMD molecules onto the fibers, it appears that some CMD detach during the harsh autoclaving conditions and/or that CMD coatings collapse during autoclaving. These hypotheses are supported by a decrease of the atomic O/C ratio following autoclaving the CMD-coated fibers.

XPS analyses of CMD-coated fibers bearing GRGDS peptides are shown in Figure 3D and Table 1. The XPS analyses showed the emission of C 1s at 286.4 and 289.0 eV, which are attributed to C—N and C—O—NH, respectively.³³ Moreover, the N 1s/C 1s ratio on samples bearing GRGDS is higher than that of CMD (Table 1), which confirms the successful immobilization of

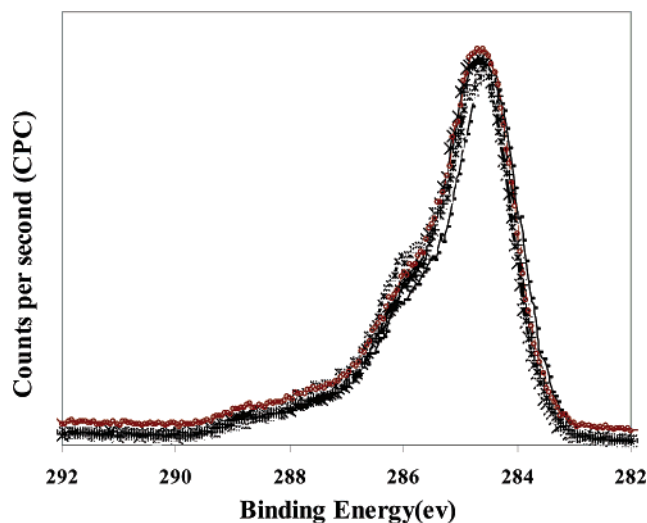


Figure 4. High-resolution XPS C 1s spectra of (○) PET + HApp + CMD (70 kDa, 1 mg/mL), (+) PET + HApp + CMD (70 kDa, 2 mg/mL), (×) PET + HApp + CMD (70 kDa, 2 mg/mL) following autoclaving, (−) PET + HApp + CMD (500 kDa, 1 mg/mL), and (*) PET + HApp + CMD (500 kDa, 2 mg/mL). CMD with a ratio of one carboxyl group to two sugar units was used. The different CMD coatings show similar C 1s spectra.

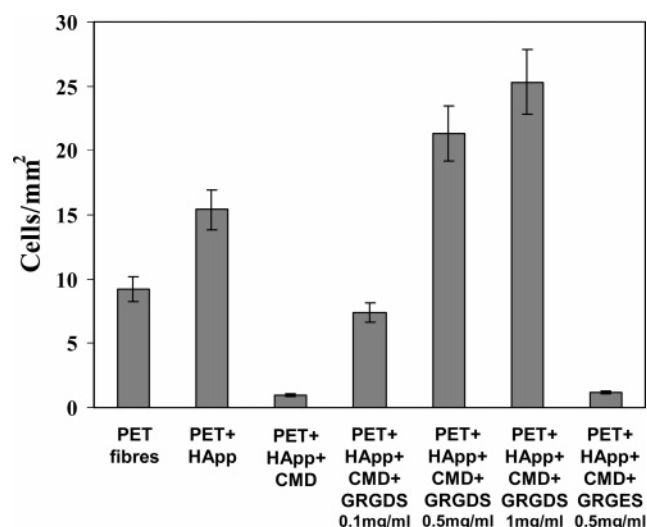


Figure 5. Endothelial cell adhesion (4 h following cell seeding) on PET fibers coated by the different layers. Error bars represent one standard deviation. A 70 kDa CMD, carboxylation degree of 1:2, and 2 mg/mL CMD solution concentration were used in these experiments. Note that surface immobilization of CMD on HApp-coated PET monofilaments significantly reduced HUVEC adhesion (1.00 ± 0.04 cells/mm²; $p < 0.05$). HApp-coated fibers: 16 ± 1 cells/mm² and GRGDS- or GRGES-bearing fibers (0.1 mg/mL GRGDS): 8.0 ± 0.3 cells/mm², (0.5 mg/mL GRGDS): 21 ± 4 cells/mm², (1 mg/mL GRGDS): 25 ± 2 cells/mm², and (0.5 mg/mL GRGES): 1.0 ± 0.2 cells/mm²; $p < 0.05$).

GRGDS on CMD-coated fibers. In addition, the atomic N/C ratio increases as the GRGDS concentration increases from 0.1 to 1 mg/mL. However, the spectral congestion made it difficult to look for small differences between C 1s signals of RGD coatings and CMD layers. As the CMD layers bearing RGD certainly collapsed during XPS analyses, cell adhesion was investigated to verify that indeed there was RGD immobilized on the CMD interlayer and to compare the effect of RGD concentration on cell responses.

Grafting the RGD peptides onto polymer surfaces, via a stable covalent amide bond, is usually performed by reacting activated surface carboxylic acid groups with the nucleophilic N-terminus

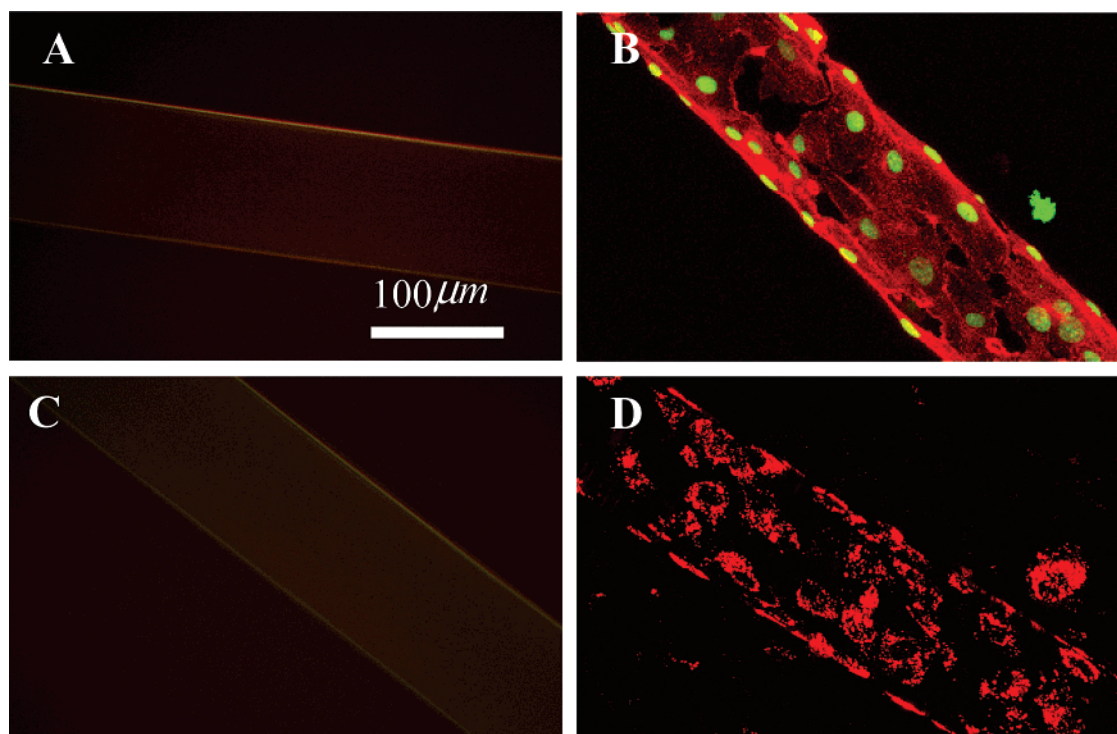


Figure 6. Confocal microscopic observations of endothelial cells at day 4 on (A) PET + HApp + CMD (70 kDa, carboxylation degree of 1:2, 2 mg/mL), (B) PET + HApp + CMD + GRGDS (0.5 mg/mL), and (C) PET + HApp + CMD + GRGES (0.5 mg/mL) and at day 8 on (D) PET + HApp + CMD + GRGDS (0.5 mg/mL). Endothelial cells were stained for nuclei with SYTOX Green Nucleic Acid Stain and for actin filaments with TRITC-phalloidin in panels A–C and with dil-acetylated LDL in panel D. Original magnification was 200 \times .

of the peptide. Carboxylic acid groups can be activated by using carbodiimide chemistry.^{11,34–36} Two problems may arise when using this coupling method. First, RGD peptides contain functional groups (e.g., carboxyl groups at the C-terminus and in the aspartic acid side chain and the nucleophilic guanidino group of the arginine side chain; see Figure 2B). Second, the coupling reagent and the activated carboxyl groups can be deactivated quickly by hydrolysis. To minimize these potential problems, we employed a two-step procedure. Surface carboxyl groups were first activated to form active esters (i.e., *N*-hydroxysuccinimide (NHS) esters), and then the peptides were coupled onto the activated carboxyl groups in phosphate buffer at pH 8. It has been reported that grafting of RGD peptides onto active ester groups available on surfaces was optimal in phosphate or sodium bicarbonate buffer at pH 8–9.^{34,37} In this study, GRGDS in three different concentrations (0.1, 0.5, and 1 mg/mL) were grafted on CMD-coated fibers by employing a two-step procedure.

Testing of Surface-Coated Fibers toward Endothelial Cell Responses. In multicellular organisms, cell–cell and cell–ECM interactions are mediated by cell adhesion receptors.¹¹ Among these receptors, the integrin family comprises the most numerous and versatile group.¹¹ Multiple integrin receptors with distinctive combinations of α and β subunits have been identified on the surface of vascular endothelial cells.^{38,39} Among them, $\alpha_5\beta_1$ and $\alpha_v\beta_3$, which bind to the ECM proteins fibronectin and vitronectin, respectively, are the best characterized and appear to be critical in the establishment and stabilization of endothelial cell monolayers. Earlier studies have shown that adhesion of endothelial cells on glass or polymeric substrates is promoted by RGD immobilization on these surfaces.^{15,16,20} The RGD peptide sequence is found in many extracellular matrix proteins (e.g., fibronectin, vitronectin, collagen, and fibrinogen) and is the binding motif for the cell attachment receptor (integrin $\alpha_v\beta_3$) present on several cell membranes. The process of integrin-

mediated cell adhesion comprises four different partly overlapping events:¹¹ (1) cell attachment, (2) cell spreading, (3) actin cytoskeleton organization, and (4) focal adhesion formation. First, in the initial attachment step, the cell makes contact with the surface and some ligand binding occurs, allowing the cell to withstand gentle shear stresses. Second, the cell body begins to flatten, and its plasma membrane spreads over the substrate. Third, actin organizes into microfilament bundles, referred to as stress fibers. Fourth, focal adhesion points form, which link the ECM to molecules of the actin cytoskeleton.¹¹

Endothelial Cell Attachment on Surface-Modified Fibers.

Cell adhesion and cell spreading assays were in good agreement with the expected results that were based on the chemical analysis and provided insight into how HUVECs respond to PET fibers covered by the different thin films. Cell adhesion was studied on all samples and expressed as cells/mm² fiber surfaces. As expected, cell adhesion was reduced on CMD-coated surfaces (Figure 5). In fact, HUVEC adhesion was the lowest on CMD-modified PET fibers, whereas HApp- and GRGDS-coated fibers promoted the highest cell adhesion (Figure 5; HApp-coated fibers: 16 ± 1 cells/mm² and GRGDS- or GRGES-bearing fibers (0.1 mg/mL GRGDS): 8.0 ± 0.3 cells/mm², (0.5 mg/mL GRGDS): 21 ± 4 cells/mm², (1 mg/mL GRGDS): 25 ± 2 cells/mm², and (0.5 mg/mL GRGES): 1.0 ± 0.2 cells/mm²; $p < 0.05$).

The HApp coating is solid and dense and therefore contributes minimal interfacial steric–entropic repulsion effects.² It also possesses a low density of positive surface charges in a pH 7.4 buffered saline solution.^{40,41} Hence, interfacial electrostatic forces are small, and protein adsorption onto the HApp layer may occur predominantly by dispersion and hydrophobic forces.^{2,40,41} Therefore, it is suggested that cell adhesion on HApp-coated surfaces, in our study, is due to serum born protein adsorption. In the case of non-coated PET fibers, the small

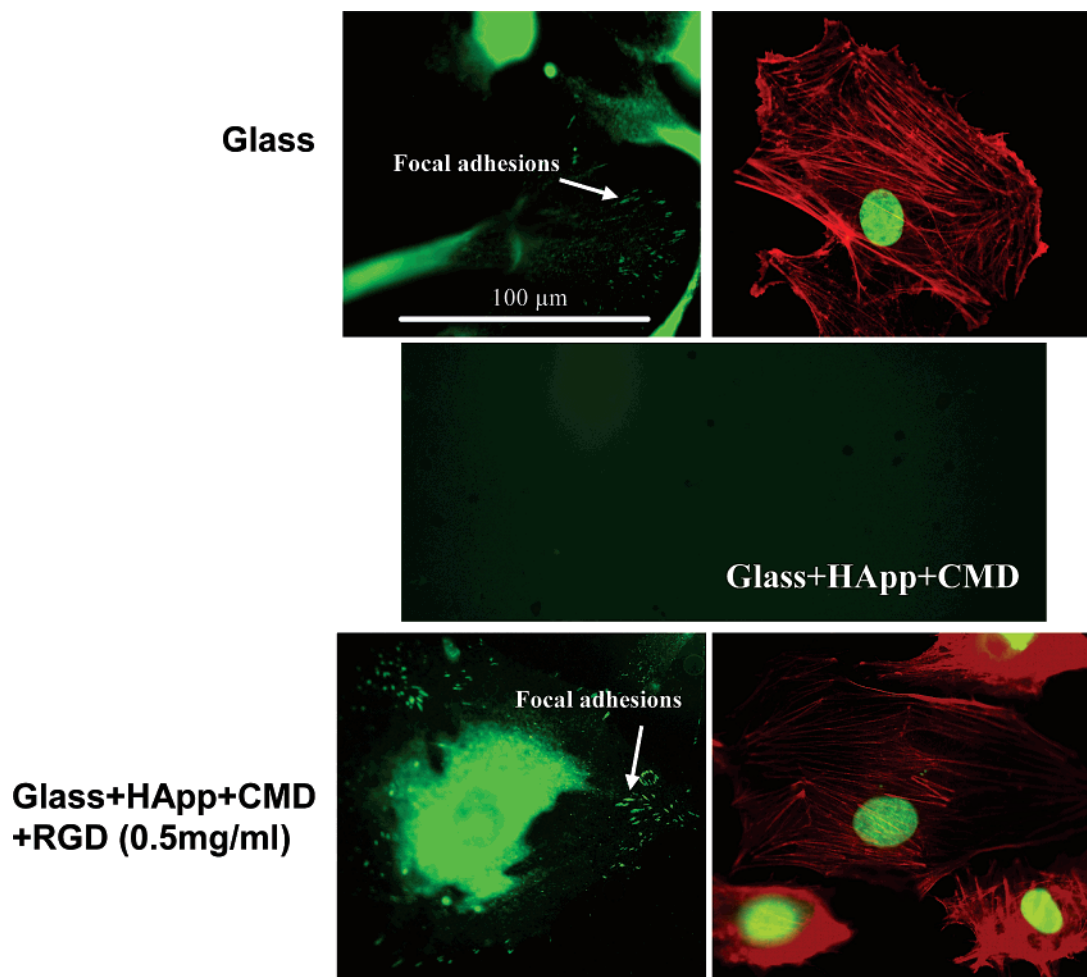


Figure 7. Images obtained by epifluorescence microscopy of the HUVECs stained for actin stress fibers (red) and vinculin (green). Original magnification was 600 \times .

amount of cell adhesion may occur due to hydrophobic and dispersion forces as described previously.

Surface immobilization of CMD on HApp-coated PET monofilaments significantly reduced HUVEC adhesion (Figure 5; 1.00 ± 0.04 cells/mm²; $p < 0.05$). It has been reported that anionic carboxylic dextrans inhibit cell proliferation, perhaps due to an inability for the cells to adsorb onto these surfaces.^{42,43} Such surface coatings might be useful for the fabrication of coatings resistant to nonspecific cell adhesion and cell colonization. A further advantage of CMD coatings is that they can be used as interlayers for the covalent immobilization of cell-adhesive glycoproteins or other specific biological signaling proteins. Such constructs enable the fabrication of systems that exquisitely possess specific biological responses since the non-adhesive CMD interlayer would limit and/or delay other nonspecific undesired biological responses.

McLean et al.³ reported that the ability of CMD coatings to resist cell colonization significantly depends upon the mode of fabrication of the CMD coating. They reported that electrostatic interfacial forces are not the dominant factors governing the cell and tissue responses. However, a minimum CMD coating thickness or coverage is required for effective antifouling. Before interpreting biological responses of surface coatings, it is, however, essential to ascertain that such interpretations are not due to artifacts superimposed on the inherent interfacial properties of the coatings. For example, the presence of gaps in the surface coating could influence the results, but these would be difficult to find. As the HApp itself is cell adhesive, data

presented in Figure 5 could be interpreted as a result of incomplete CMD coverage and/or a too thin CMD layer. The CMD coating grafted onto the HApp layer may therefore be seen as a carpet pile structure as described elsewhere,³ in which polysaccharide chains are randomly attached by multiple pinning points and contain protruding loops and chain ends as well as trains (chain lengths that are pinned close to the surface). Loops and tail ends extend into the aqueous solution away from the solid surface because of their high solubility in water and the drive for charged groups to spread out away from the interface. Such protruding loops and chain ends provide steric–entropic hindrance to protein adsorption and cell attachment.^{2,3} The very low cell adhesion observed on CMD-coated fibers indicates that such steric–entropic repulsive interfacial forces were present. Yet, the small amount of cell adhesion observed in our study indicates that the magnitude of the repulsive steric–entropic forces was not sufficient to completely overcome the attractive interfacial forces. But, these coatings were capable of limiting these nonspecific adsorption events to allow the RGD surfaces to specifically control the cell responses.

Surface grafting of GRGDS peptides on CMD-coated PET monofilaments promoted cell adhesion at levels significantly higher than those observed on CMD-coated fibers. Also, cell adhesion significantly depended on the GRGDS solution concentration used during the grafting procedure (Figure 5; GRGDS-bearing fibers (0.1 mg/mL GRGDS): 8.0 ± 0.3 cells/mm², (0.5 mg/mL GRGDS): 21 ± 4 cells/mm², and (1 mg/mL GRGDS): 25 ± 2 cells/mm²; $p < 0.05$). Moreover, cell

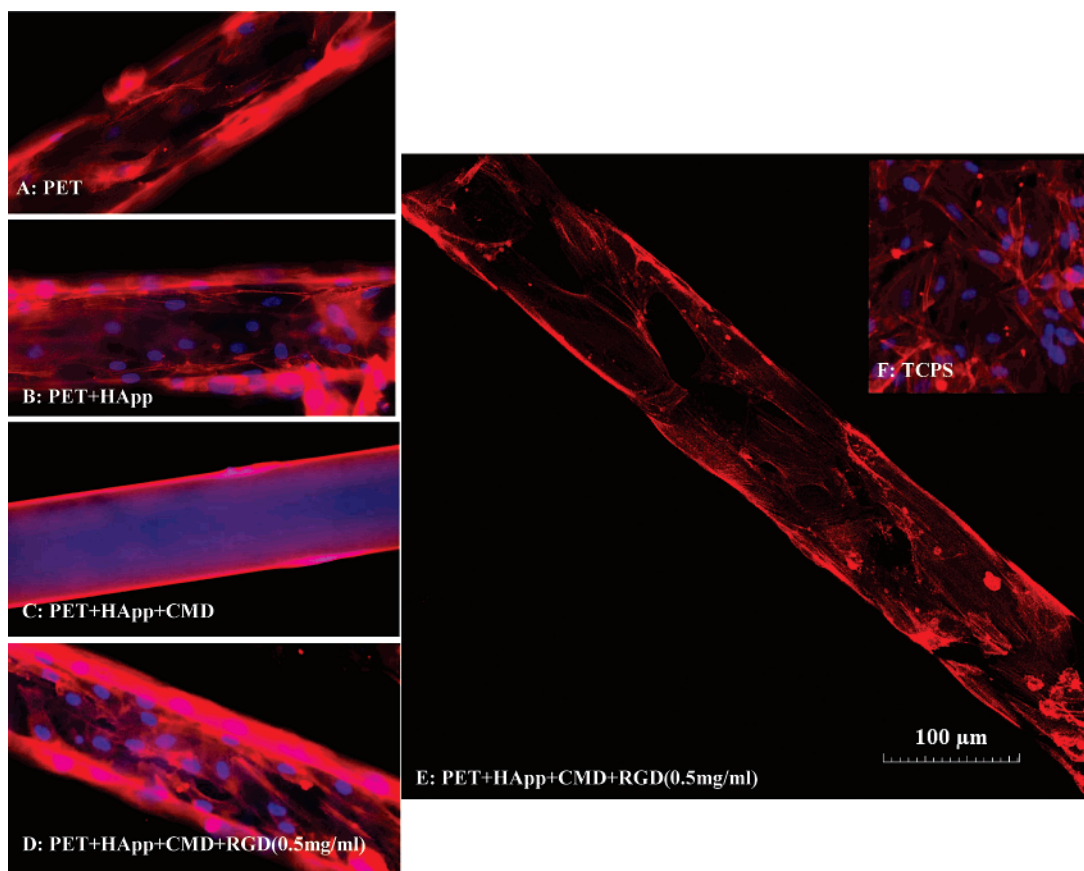


Figure 8. Epifluorescence microscope images of HUVEC spreading and orientation along the PET fiber axis (A–D) as compared to HUVEC spreading on the TCPS (F). Confocal microscope image of actin filament orientation along the fiber axis (F). Original magnification was 200 \times .

adhesion on the GRGES (inactive control, Figure 5; 1.0 ± 0.2 cells/mm 2 ; $p < 0.05$) was significantly lower than the amounts observed on GRGDS-bearing samples. These results suggest that the significant gains in endothelial cell adhesion on PET fibers bearing surface grafted GRGDS were due to the biospecific responses of HUVEC surface integrins toward the GRGDS ligands available on the fiber surfaces. Thus, cell adhesion was predominantly modulated by the incorporation of adhesion-promoting components on the fiber surface rather than random adsorption of serum-borne cell-adhesive proteins. The small amount of cell adhesion observed on nonspecific surfaces bearing immobilized GRGES peptide sequences may be supported by the previous hypotheses postulated to explain the very small amount of cell adhesion observed on CMD-coated fibers (i.e., incomplete coverage of the HApp-coated surface by CMD layer). Also, GRGES-coated fibers might contribute to some electrostatic forces that would attract proteins and cells.

The small cell adhesion observed on GRGDS-coated fibers produced using the 0.1 mg/mL GRGDS solution could be explained by the presence of an insufficient surface density of RGD molecules. This is supported by a low surface concentration of nitrogen found in XPS analyses of these RGD coatings (i.e., 0.1 mg/mL). It is possible that the GRGDS molecules are much smaller than the extended chains of the CMD layer. In this case, CMD chains could act as a cover for the small GRGDS molecules available in such a low density. CMD loops and chain ends would provide steric–entropic hindrance for the cells to access the RGD molecules when available in such a low density. This is in agreement with another study in which reduced cell attachment was observed when the spacer moiety was too long.⁴⁴ It was claimed that reduced cell attachment was not only because of the increasing entropy of the longer flexible spacer chains

that oppose strong binding⁴⁵ but also because cells would prefer somehow a tight binding to more rigid surfaces.⁴⁶ RGD peptides located at the end of flexible spacing moieties increased cell binding activity that may be caused by local enrichment of ligands.⁴⁷ To obtain a reasonable number of adherent cells on the samples, a concentration of 0.5 mg/mL GRGDS was chosen for the following experiments.

Effect of Surface-Modified Fibers on Endothelial Cell Spreading and Patterning. Cell morphology is one of the criteria used to study cell adhesion events and cell spreading.^{25,30} To observe the effect of the fiber surface chemistry on HUVEC spreading, HUVECs were double-stained to identify the cell cytoskeleton (i.e., actin filaments) and nuclei. According to the results obtained by day 4, it seems that endothelial cell adhesion, stability, and spreading depend on the surface chemistry of the samples (see Figures 6 and 7). Figure 6 shows the degree of attachment and spreading of endothelial cells on surface-modified PET fibers at day 4. Despite some cell adhesion on the CMD-coated fibers (Figure 5; 1.00 ± 0.04 cells/mm 2) and GRGES-coated fibers (Figure 5; 1.0 ± 0.2 cells/mm 2) at 4 h, no cells remained on these surfaces by day 4 (Figure 6A,C, respectively). It can be hypothesized that early cells deposited on these CMD surfaces can detach because of insufficient adhesion and spreading. In contrast, cells were confluent and largely spread on GRGDS-coated fibers (Figure 6B). These observations suggest that GRGDS-coated fibers facilitate cell adhesion and that cell spreading through their integrins toward the GRGDS ligands is available on the fiber surfaces.

Dil-Acetylated LDL Staining. To clarify if GRGDS coating is stable under cell culture conditions for a longer period of time, HUVECs were seeded on the GRGDS-coated fibers (0.5 mg/mL GRGDS concentration) and maintained in culture for a

period of 8 days. At day 2, cells were stained with dil-acetylated LDL, and daily observation with phase contrast and confocal microscopy showed the uniform cell distribution (Figure 6D), growth, and stability over the fiber surface.

Actin Stress Fibers and Focal Adhesions. Few studies have investigated endothelial cell adhesion in terms of actin cytoskeleton and focal adhesions on the surface-coupled-adhesive RGD peptide.⁴⁸ As actin stress fibers and focal adhesions are critical for cell survival,¹¹ HUVECs were seeded on uncoated, HApp + CMD- and HApp + CMD + RGD-coated glass substrates to study the effect of these coatings on actin stress fibers and focal adhesions. In Figure 7, the red and green staining denotes actin stress fibers and focal adhesion points, respectively. As expected, there was no cell on the CMD-coated surfaces to be observed for actin stress fibers and for focal adhesions. The sharp focal vinculin staining noted on RGD-coated substrates was absent on uncoated glass. Also, actin staining was intense on RGD-coated surfaces when compared to the uncoated glass (Figure 7). This observation demonstrates the bioactivity of RGD-coated substrates. It also shows that the RGD peptides were strongly surface immobilized on the solid substrates, which is essential to promote strong cell adhesion because formation of focal adhesions only occurs if the ligands can withstand cell contractile forces.¹¹

Cell Elongation along the Fiber Axis. To observe the effect of the fiber curvature and fiber surface chemistry on HUVEC spreading and orientation in long-term cell cultures (i.e., 10 days), HUVECs were double-stained with TRITC-phalloidin for the cell cytoskeleton (i.e., actin filaments) and with Hoechst 33258 for nuclei. Epifluorescence microscopy observations showed that, on untreated PET fibers and on HApp- and GRGDS-coated fibers, cell bodies were elongated along the fiber axis (Figure 8A,B,D) as compared to those observed on the flat surfaces of the tissue culture polystyrene plates (Figure 8F), which were randomly spread. Confocal microscopy photographs show that actin filaments were oriented parallel to the fiber axis; Figure 8E shows a typical image illustrating this effect. Cell orientation along the fiber can be influenced by fiber curvature as previously reported that most cell types are known to orient and often move rapidly along fibers in the 5–108 μm range.^{5,7} More investigations will be warranted to better understand how fiber curvature and fiber diameter can affect cell responses.

Conclusion

Bioactive polymer fibers that encourage and control directional biological responses were developed, characterized, and validated. For this purpose, RGD peptide, a cell-adhesive sequence, was selected and immobilized onto the surface of PET fibers (monofilaments), using a plasma polymer layer and a low-fouling and non-adhesive carboxy-methyl-dextran interlayer to modulate endothelial cell patterning in a 3-D environment. Bioactivated fibers could be used to modulate cell patterning when dispersed in a 3-D environment.

X-ray photoelectron spectroscopy (XPS) analyses enabled detailed characterization of the multilayer fabrication steps. Human umbilical vein endothelial cells (HUVEC) were used to investigate cell patterning (i.e., adhesion, growth, spreading, and orientation) as a function of the fiber surface properties. As expected, cell adhesion was reduced on CMD-coated fibers as HUVEC adhesion was the lowest on these fibers, whereas amine- and GRGDS-coated fibers promoted cell adhesion, growth, and spreading. These low-fouling CMD surface coatings (and possibly other low-fouling coatings not tested in this study)

on polymer fibers could lead to the development of well-defined surface modifications that allow for the precise control of directional cellular interactions at the tissue–biomaterial interface and ultimately improved performance of long-term biomaterial implants. Moreover, cell adhesion on the GRGES-coated fibers (nonactive peptide control) was significantly lower than that observed on GRGDS-coated fibers. These observations suggest that the significant gains in endothelial cell adhesion on PET fibers bearing surface grafted GRGDS were due to the biospecific responses of cell surface integrins toward RGD ligands available on the fiber surfaces. Cell adhesion increased by increasing GRGDS concentration. Cells on RGD-coated substrates formed well-defined stress fibers and sharp spots of vinculin, typical of focal adhesions. However, further studies will have to be undertaken to investigate in more detail the effect of RGD peptide surface density on cell responses. In addition, fiber patterns promoted cell orientation along the fiber axis in comparison to flat surfaces, and this parameter was more effective in long-term cell cultures.

Acknowledgment. This study was supported by Sherbrooke University (P.V.), NSERC Individual Research Grant (P.V.), Fonds FCAR Strategic Grant (P.V.), and FQRNT Projet de Recherche en Équipe (P.V., C.J.D., and A.H. (MSRT)). The authors are grateful to Julie Chouinard, Emmanuelle Monchaux, Laurie Martineau, and Marc G. Couture for their useful comments and technical assistance.

References and Notes

- McLean, K. M.; McArthur, S. L.; Chatelier, R. C.; Kingshott, P.; Griesser, H. J. *Colloids Surf., B* **2000**, *17* (1), 23–35.
- McArthur, S. L.; McLean, K. M.; Kingshott, P.; St. John, H. A. W.; Chatelier, R. C.; Griesser, H. J. *Colloids Surf., B* **2000**, *17* (1), 37–48.
- McLean, K. M.; Johnson, G.; Chatelier, R. C.; Beumer, G. J.; Steele, J. G.; Griesser, H. J. *Colloids Surf., B* **2000**, *18* (3–4), 221–34.
- Wong, J. Y.; Leach, J. B.; Brown, X. Q. *Surf. Sci.* **2004**, *570* (1–2), 119–33.
- Curtis, A.; Riehle, M. *Phys. Med. Biol.* **2001**, *46* (4), 47–65.
- Barbucci, R.; Lamponi, S.; Magnani, A.; Pasqui, D. *Biomol. Eng.* **2002**, *19* (2–6), 161–70.
- Khang, G.; Lee, S. J.; Lee, J. H.; Lee, H. B. *Korean Polym. J.* **1999**, *7* (2), 102–7.
- Miller, D. C.; Thapa, A.; Haberstroth, K. M.; Webster, T. G. *Mater. Res. Soc. Symp. Proc.* **2002**, *711*, 201–4.
- Unger, R. E.; Peters, K.; Wolf, M.; Motta, A.; Migliaresi, C.; Kirkpatrick, C. J. *Biomaterials* **2004**, *25* (21), 5137–46.
- Maheshwari, G.; Brown, G.; Lauffenburger, D. A.; Wells, A.; Griffith, L. G. *J. Cell. Sci.* **2000**, *113* (10), 1677–86.
- Hersel, U.; Dahmen, C.; Kessler, H. *Biomaterials* **2003**, *24* (24), 4385–415.
- Johansson, B. L.; Larsson, A.; Ocklind, A.; Ohrlund, A. *J. Appl. Polym. Sci.* **2002**, *86* (10), 2618–25.
- Alcantar, N. A.; Aydil, E. S.; Israelachvili, J. N. *J. Biomed. Mater. Res.* **2000**, *51* (3), 343–51.
- Radomski, J. S.; Jarrell, B. E.; Pratt, K. J.; Williams, S. J. *Surg. Res.* **1989**, *47* (2), 173–7.
- Massia, S. P.; Stark, J. J. *Biomed. Mater. Res.* **2001**, *56* (3), 390–9.
- Kouvroukoglou, S.; Dee, K. C.; Bizios, R.; McIntire, L. V.; Zygourakis, K. *Biomaterials* **2000**, *21* (17), 1725–33.
- Vermette, P.; Meagher, L. *Langmuir* **2002**, *18* (26), 10137–45.
- Agostino, R. D. *Plasma deposition, treatment, and etching of polymers*; Academic Press: New York, 1990.
- Martin, Y.; Boutin, D.; Vermette, P. *Thin Solid Films*, in press.
- Gao, C. Y.; Guan, J. J.; Zhu, Y. B.; Shen, J. C. *Macromol. Biosci.* **2003**, *3* (3–4), 157–62.
- Morpurgo, M.; Bayer, E. A.; Wilchek, M. J. *Biochem. Biophys. Methods* **1999**, *38* (1), 17–28.
- Lofas, S.; Johnsson, B. *J. Chem. Soc., Chem. Commun.* **1990**, *21*, 1526–8.
- Jaffe, E. A.; Nachman, R. L.; Becker, C. G.; Minick, C. R. *J. Clin. Invest.* **1973**, *52* (11), 2745–56.

- (24) Neumann, T.; Hauschka, S. D.; Sanders, J. E. *Tissue. Eng.* **2003**, *9* (5), 995–1003.
- (25) Sirois, E.; Charara, J.; Ruel, J.; Dussault, J. C.; Gagnon, P.; Doillon, C. J. **1998**, *19* (21), 1925–34.
- (26) Sirois, E.; Cote, M. F.; Doillon, C. J. *Int. J. Artif. Organs* **1993**, *16* (8), 609–19.
- (27) Wen, C. H.; Chuang, M. J.; Hsiue, G. H. *Appl. Surf. Sci.* **2006**, *252* (10), 3799–805.
- (28) Gengenbach, T. R.; Chatelier, R. C.; Griesser, H. J. *Surf. Interface Anal.* **1996**, *24* (4), 271–81.
- (29) Griesser, H. J.; Chatelier, R. C. *J. Appl. Polym. Sci.* **1990**, *46*, 361–84.
- (30) Terlingen, J. B. A.; Hoffman, A.; Feijen, J. Plasma modification of polymeric surfaces for biomedical applications. In *Advanced biomaterials in biomedical engineering and drug delivery systems*; Ogata, N. K. S., Feijen, J., Okano, T., Eds.; Springer-Verlag: New York, 1996.
- (31) Gengenbach, T. R.; Vasic, Z. R.; Chatelier, R. C.; Griesser, H. J. *J. Polym. Sci., Part A: Polym. Chem.* **1994**, *32* (8), 1399–414.
- (32) Vermette, P.; Gengenbach, T.; Divisekera, U.; Kambouris, P. A.; Griesser, H. J.; Meagher, L. J. *Colloid Interface Sci.* **2003**, *259* (1), 13–26.
- (33) Porte-Durrieu, M. C.; Labrugere, C.; Villars, F.; Lefebvre, F.; Dutoya, S.; Guette, A. et al. *J. Biomed. Mater. Res.* **1999**, *46* (3), 368–75.
- (34) Hern, D. L.; Hubbell, J. A. *J. Biomed. Mater. Res.* **1998**, *39* (2), 266–76.
- (35) Rezaia, A.; Johnson, R.; Lefkow, A. R.; Healy, K. E. *Langmuir* **1999**, *15* (20), 6931–9.
- (36) Xiao, S. J.; Textor, M.; Spencer, N. D.; Sigrist, H. *Langmuir* **1998**, *14* (19), 5507–16.
- (37) Besselink, G. A. J.; Beugeling, T.; Bantjes, A. *Appl. Biotechnol.* **1993**, *43* (3), 227–46.
- (38) Albelda, S. M.; Daise, M.; Levine, E. M.; Buck, C. A. *J. Clin. Invest.* **1989**, *83* (6), 1992–2002.
- (39) Luscinskas, F. W.; Lawler, J.; *FASEB J.* **1994**, *8* (12), 929–38.
- (40) Chatelier, R. C.; Drummond, C. J.; Chan, D. Y. C.; Vasic, Z. R.; Gengenbach, T. R.; Griesser, H. J. *Langmuir* **1995**, *11* (10), 4122–8.
- (41) Chatelier, R. C.; Hodges, A. M.; Drummond, C. J.; Chan, D. Y. C.; Griesser, H. J. *Langmuir* **1997**, *13* (11), 3043–6.
- (42) Hartley, P. G.; McArthur, S. L.; Mclean, K. M.; Griesser, H. J. *Langmuir* **2002**, *18* (7), 2483–94.
- (43) Letourneur, D.; Logeart, D.; Avramoglou, T.; Jozefonvicz, J. *J. Biomater. Sci., Polym. Ed.* **1993**, *4* (5), 431–44.
- (44) Beer, J. H.; Springer, K. T.; Collier, B. S. *Blood* **1992**, *79* (1), 117–28.
- (45) Wong, J. Y.; Kuhl, T. L.; Israelachvili, J. N.; Mullah, N.; Zalipsky, S. *Science* **1997**, *275* (5301), 820–2.
- (46) Pelham, R. J.; Wang, Y. L. *Biol. Bull.* **1998**, *194* (3), 348–9.
- (47) Mammen, M.; Choi, S. K.; Whitesides, G. M. *Angew. Chem., Int. Ed.* **1998**, *37* (20), 2755–94.
- (48) Massia, S. P.; Hubbell, J. A. *J. Biomed. Mater. Res.* **1991**, *25*, 223–42.

BM060957F